# Grid sense multiple access

## A decentralized control algorithm for DC grids

van der Blij, Nils H.; Ramirez-Elizondo, Laura M.; Spaan, Matthijs T.J.; Bauer, Pavol

**DOI**
10.1016/j.ijepes.2020.105818

**Publication date**
2020

**Document Version**
Final published version

**Published in**
International Journal of Electrical Power and Energy Systems

Electrical Power and Energy Systems 119 (2020) 105818

Contents lists available at ScienceDirect

Electrical Power and Energy Systems

journal homepage: www.elsevier.com/locate/ijepes

# Grid sense multiple access: A decentralized control algorithm for DC grids☆

Nils H. van der Blij*, Laura M. Ramirez-Elizondo, Matthijs T.J. Spaan, Pavol Bauer

*Delft University of Technology, Delft 2600 AA, the Netherlands*

ARTICLE INFO

*Keywords:*
Algorithm
Control
Dc grids
Decentralized
Energy utilization

ABSTRACT

Due to the distributed nature of future electrical power systems, decentralized control is essential for these grids. This paper shows that converters that have identical voltage thresholds switch off simultaneously even if some could have remained operational. Therefore, inadequate system and energy utilization can occur when decentralized demand or supply response is utilized. The Grid Sense Multiple Acces (GSMA) algorithm proposed in this paper ensures that, after a change occurs in the system, a subset of the converters remains connected to the grid, without the need of utilizing any form of communication. This is achieved by introducing an exponential backoff time between failed connection attempts. Furthermore, several simulations and experiments are conducted to illustrate and validate the behavior of the GSMA algorithm, showing that it can be applied to dc grids in order to improve system and energy utilization.

## 1. Introduction

The increasing presence of distributed energy resources, the introduction of microgrids, and the increasing number of prosumers (participants that both produce and consume) subject the electrical power grid to considerable changes. These changes pose significant challenges to the control and management of these grids [1–3].

Traditionally, electrical power grids have had a centralized and radial structure. However, the centralized structure and control methods used for traditional systems are not adequate for systems where generation is distributed. Thus, different system topologies and control architectures are called for to facilitate bi-directional power flow and the segmentation of the grid [3–7].

The increasing share of solar and wind energy generation results in a significant reduction of the inertia of electrical power grids. Furthermore, the segmentation of the grid into, for example, microgrids is increasing. Accordingly, the power management and control strategies of these grids need to be adapted to ensure the balance of supply and demand on shorter time scales and for varying system topologies [8–12].

Because of the distributed nature of future electrical power grids, it is often not desirable to use communication. Furthermore, for systems with a communication infrastructure, it is preferable that the system sustains operation when there is a communication malfunction. Therefore, decentralized control is essential for future electrical power grids [13,14].

Previous work presents several decentralized strategies to ensure stability, power quality and power sharing for smart grids. Droop based control strategies are commonly used for many systems [15–17]. Further efforts improve power quality and stability by adapting the converters' virtual impedance or operating mode depending on measured parameters [18–20]. Moreover, several plug-and-play strategies are presented [21–23]. Often, an overarching hierarchical control is used to control the power flow [24–27].

Decentralized control strategies often implement demand and supply response based on local measurements. It is shown in this paper that, when voltage dependent demand and supply response is implemented in dc systems with converters that exhibit discrete behavior (that do not ramp their output power, but switch on or off entirely), the system and energy utilization can become inadequate. In these cases it must be determined, with or without communication, which subset of the converters remain operational in order to improve system and energy utilization.

This paper has several distinct contributions. First, it is experimentally shown that inadequate system and energy utilization can occur for decentralized control with discrete behavior. Second, the Grid Sense Multiple Access algorithm is proposed to improve system and energy utilization, without employing communication. The algorithm

☆ This project has received funding in the framework of the joint programming initiative ERA-Net Smart Grids Plus, with support from the European Union's Horizon 2020 research and innovation programme.

* Corresponding author.
*E-mail addresses:* N.H.vanderBlij@TUDelft.nl (N.H. van der Blij), L.M.RamirezElizondo@TUDelft.nl (L.M. Ramirez-Elizondo), M.T.J.Spaan@TUDelft.nl (M.T.J. Spaan), P.Bauer@TUDelft.nl (P. Bauer).

https://doi.org/10.1016/j.ijepes.2020.105818
Received 3 June 2019; Received in revised form 18 December 2019; Accepted 3 January 2020

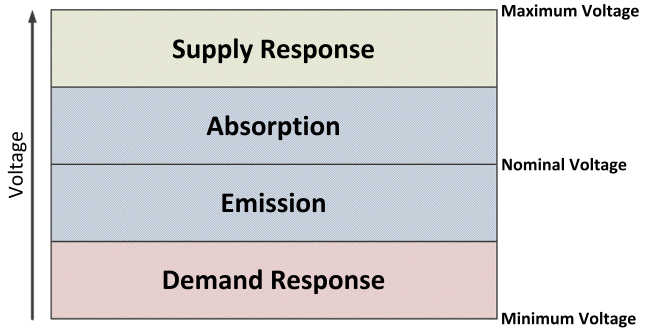


**Fig. 1.** Supply response, absorption, emission and demand response voltage regions for the decentralized control of dc smart grids.

enables a subset of the converters to remain connected to the grid, by introducing an exponential backoff time between connection attempts. Third, it is shown that the priority of the converters and behavior of the algorithm can be influenced by altering the algorithm's parameters. Last, several simulations and experiments are conducted to validate and illustrate the behavior of the GSMA algorithm.

The remainder of this paper is organized as follows: In Section 2, a challenge related to the energy utilization in dc smart grids is discussed. In Section 3, the Grid Sense Multiple Access algorithm is proposed. In Section 4, several simulations are performed to illustrate the behavior of the GSMA algorithm. In Section 5, the behavior of the GSMA algorithm is further validated by conducting four experiments. Finally, in Section 6, conclusions are drawn.

## 2. Background: Decentralized control and discrete behavior

To ensure stability and power quality of dc grids, the voltages between the maximum and minimum allowed voltage are divided into supply response, absorption, emission and demand response regions, as is shown in Fig. 1 [21]. In the supply and demand response regions, the respective sources and loads are disconnected before the maximum or minimum voltage is reached. This is done to prevent the voltage from exceeding the maximum voltage or becoming less than the minimum voltage, but also to ensure stability. The change in output power can either be ramped or abruptly switched at a specified voltage.

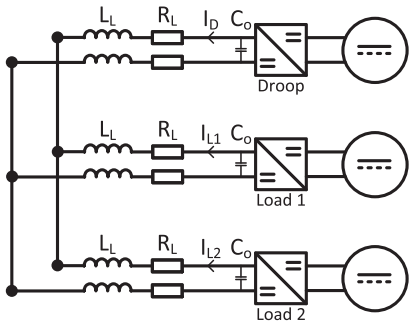


**Fig. 2.** Schematic of the experimental dc microgrid set-up consisting of one droop controlled converter and two constant power controlled converters.

### 2.1. Sources and loads with discrete behavior

Sources and loads, such as photovoltaic panels and resistive heating, can easily ramp their output power. However, not all applications have that capability. Furthermore, many current standards indicate a fixed voltage to switch off, instead of a region over which it can be ramped. They exhibit so-called discrete behavior, since these sources and loads can only switch on or off.

For the sources and loads with discrete behavior, the voltage at which it is disconnected determines its priority. In larger systems such as distribution systems, it is likely that there are multiple converters present with the same priority. For example, multiple houses in a neighbourhood with photovoltaic panels, or multiple street lights in a street lighting system.

The combination of this form of decentralized control and discrete behavior can reduce the energy utilization in smart grids. To illustrate this, a dc system consisting of a photovoltaic panel and two loads, which are switched off at a specified voltage, is investigated. When the photovoltaic panel is only producing enough power to supply one load, the voltage will eventually drop below the voltage threshold and both loads will switch off. However, in this case one of the loads could have remained operational.

### 2.2. Experimental results for loads with discrete behavior

To demonstrate this behavior, the example of the previous subsection was implemented in the experimental set-up shown in Fig. 2. The set-up is discussed in more detail in Section 5, but in essence it consists of a droop controlled converter and two constant power load controlled converters.

The droop converter is first operating with a reference voltage of 350 V and a droop constant of 250 W/V, while the two load converters are consuming a constant power of 2.5 kW and switch off when the voltage drops below 325 V. The output voltage of the droop converter and the output currents of the converters, when at t = 0.1 s the droop constant is reduced to 125 W/V, are shown in Fig. 3. Observe that both loads detect an undervoltage and switch off, although one of the loads could have consumed 2.5 kW without the voltage dropping below 325 V. Ideally, only one load should switch off, while the other remains operational. However, since no central controller or communication link is available to ensure that one of the loads remains operational, the system and the available energy are not fully utilized.

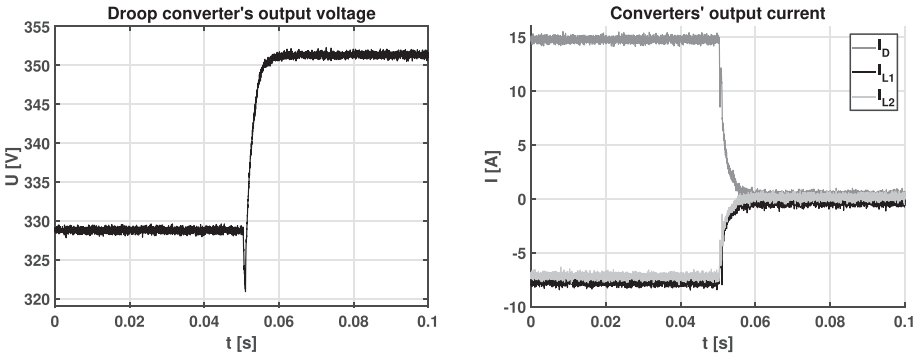


**Fig. 3.** Experimental results for two identical loads with discrete behavior and a reduction in the droop converter's droop constant.

## 3. Grid sense multiple access algorithm

The previous section showed that converters, which have identical priority and exhibit discrete behavior, can cause inadequate system and energy utilization. Intuitively, a simple solution might seem to re-connect the converters when the voltage crosses a certain threshold. However, even if the number of connection attempts are limited, both converters detect the same number of failures and eventually both abort attempting connection.

The Grid Sense Multiple Access Voltage Detection (GSMA/VD) algorithm is proposed, which is inspired by the Carrier Sense Multiple Access Collision Detection (CSMA/CD) algorithm, used for local area networking in the beginning of Ethernet [28]. In the CSMA/CD algorithm, data is only sent if the carrier is available and, when a collision is detected during transmission, a jamming signal is sent and the sender waits for a random time interval before re-attempting transmission. Similarly, in the GSMA/VD algorithm, converters only connect to a grid when the voltage is above its threshold and, when an undervoltage is detected during connection, the connection is aborted and the converter waits for a random time before re-attempting connection.

The GSMA algorithm uses exponential backoff to make it unlikely that different converters repeatedly attempt reconnection simultaneously. When a converter is connected to the grid, its number of connection attempts $N$ is set to the start value $S$ and the converter is put in an off state. From the off state, if the number of attempts is less than the maximum number of attempts $K$, the voltage at the converter's output is measured until an acceptable level is reached. Subsequently, the converter will wait a random time between 0 and $\tau \cdot E^N$, where $\tau$ is the base time constant and $E$ is the exponential base. Afterwards, the number of attempts is incremented and the converter is switched on. Finally, the grid is continuously sensed and the converter is disconnected if the voltage threshold is crossed. Furthermore, the number of attempts is set to the reset value $R$ if the converter remains successfully connected for at least the reset time $T_r$. The Grid Sense Multiple Access/Voltage Detection (GSMA/VD) for loads in dc grids is shown in Fig. 4, but a similar approach can be used for source converters.

### 3.1. GSMA/VD parameters

The GSMA/VD parameters, which are used for the simulations and experiments in this paper, are summarized in Table 1. In this subsection, the significance of these parameters is discussed, but the optimization of the exponential backoff component of the GSMA/VD algorithm is beyond of the scope of this paper, partly because it is dependent on the system and application of the algorithm [29,30].

The base time constant $\tau$ determines the time scaling of the control algorithm, which will mostly be determined by the response time of the system. The dc grids in this paper have a total capacitance of around 1 mF, and a droop impedance of maximally 1 Ω. Therefore, the RC time constants of these systems are around 1 ms.

The reset time $T_r$ determines when a connection attempt is deemed successful. Therefore, $T_r$ should be significantly larger than the base time constant to ensure than the system has reached steady-state, but as low as possible to speed up the decision making process. In this paper, a conservative reset time of 25 ms is chosen.

The exponential base $E$ dictates how quickly the waiting time increases for consecutive connection attempts. A high base reduces the number of connection attempts as the waiting time increases rapidly, increasing the chance of reaching the reset time. However, the probability of long decision making times are relatively high. On the other hand, a low base generally ensures lower overall decision making times, but may result in many failed connection attempts. Since the objective of the algorithm is to improve energy utilization, and the fluctuations in voltage are deemed acceptable, a base of 2 is chosen.

The start parameter $S$ and the reset parameter $R$ determine if the algorithm prioritizes converters that are attempting connection, or converters that are already successfully connected. If $S < R$ connecting converters have priority over already connected converters, when $S = R$ all converters have equal priority, and when $S > R$ connected converters have priority. Assuming the priority of connected converters and an exponential base of 2, $S$ is chosen as 3 and $R$ is chosen as 1. In this case, the probability that the connected converters reach the reset time in one of the attempts before the connecting converters is high.

The maximum number of attempts $K$ determines how many attempts the converter will take, before connection will be aborted. $K$ must be large enough to make the probability that a converter incorrectly aborts is sufficiently small. However, smaller values of $K$ reduce the number of voltage fluctuations (caused by the failed attempts) and therefore improve the power quality of the system. In this paper, $K$ is chosen as 8, leading to a final connection attempt with a random time between 0 and 256 ms, making it likely one of the converters reaches the reset time.

The factor $\alpha$ regulates the hysteresis margin between the voltage at which the converter is disconnected and the voltage at which the converter attempts connection. For loads, the voltage margin $\alpha$ is always equal to or larger than 1, while for sources $\alpha$ is always equal to or lower than 1. In this paper, hysteresis is not used, and therefore $\alpha$ is chosen to be 1.

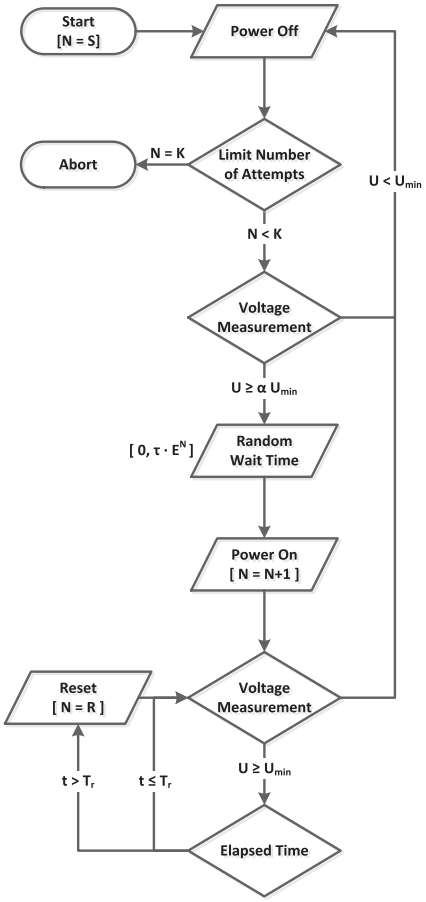


**Fig. 4.** The Grid Sense Multiple Access Voltage Detection (GSMA/VD) algorithm for loads in dc smart grids with discrete behavior.

**Table 1**
GSMA/VD parameters, which are used in the simulations and experiments.

| $\tau$ [ms] | $T_r$ [ms] | $E$ | $S$ | $R$ | $K$ | $\alpha$ |
|---|---|---|---|---|---|---|
| 1 | 25 | 2 | 3 | 1 | 8 | 1 |

### 3.2. Advantages and challenges of GSMA

The GSMA algorithm yields several advantages. First, the algorithm is suitable for grids which (temporarily) do not have a communication infrastructure. Second, the priority of loads and sources is still primarily determined by the chosen voltage at which the converter disconnects. Third, the priority between connected converters and connecting converters with the same thresholds can be selected via $R$ and $S$. Last, when converters have equal priority, it is randomly decided which subset of converters remain connected to the grid.

There are also a few challenges related to the GSMA algorithm. First, due to the local measurement of the grid, the priorities of the converters can be distorted due to the effects of the grid topology. However, this is not a consequence of the algorithm but a general consequence of decentralized control. Second, although fluctuations do not occur endlessly, up to $K$ fluctuations occur for every significant change in the system where a decision must be made. Nevertheless, the fluctuations occur within the set minimum and maximum voltage. Third, during the decision-making process (which takes up to $\tau E^{K+1}$), converters equal in priority can experience intermittent operation. For the chosen parameters, a decision is made within 500 ms.

## 4. GSMA/VD simulation examples

In this section several simulations are performed to illustrate the behavior of the GSMA/VD algorithm. In this section a reduction in droop constant mostly causes the need for demand response. However, changes in system topology, generation or consumption can also provoke supply or demand response.

### 4.1. State-Space simulation model for DC smart grids

Fig. 5 shows an example of a bipolar dc system. Every dc system can be modelled by its $n$ nodes, $l$ (distribution) lines and $o$ phase conductors. In this paper, the lines are modeled using a lumped element $\pi$ model.

The state variables for the state-space system model are chosen to be the currents flowing in each line and the voltages at each node. The node voltages are related to the nodes' capacitances and the net currents flowing into each node, and the line currents are related to the voltages over the lines' inductances. Therefore, the differential equations for the state-space model are given by

$$\boldsymbol{C}\dot{\boldsymbol{U}}_{\boldsymbol{N}} = \boldsymbol{I}_{\boldsymbol{N}} - \boldsymbol{\Gamma}^{\boldsymbol{T}}\boldsymbol{I}_{\boldsymbol{L}}, \tag{1}$$

$$\boldsymbol{L}\dot{\boldsymbol{I}}_{\boldsymbol{L}} = \boldsymbol{\Gamma}\boldsymbol{U}_{\boldsymbol{N}} - \boldsymbol{R}\boldsymbol{I}_{\boldsymbol{L}}, \tag{2}$$

where $\boldsymbol{U_N}$ are the node voltages, $\boldsymbol{I_L}$ are the line currents, $\boldsymbol{I_N}$ are the currents flowing from converters into each node, $\Gamma$ is the incidence matrix, and $\boldsymbol{C}$, $\boldsymbol{L}$ and $\boldsymbol{R}$ are the capacitance, inductance and resistance matrices of respectively [31].

For the simulation the bipolar dc smart grid shown in Fig. 5 is used.

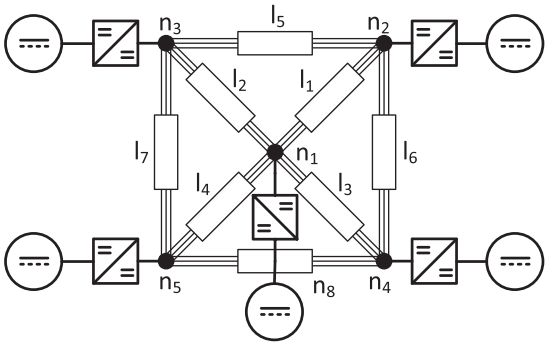


**Fig. 5.** Example dc system for the simulations of the GSMA/VD algorithm.

**Table 2**
Line parameters for the simulations of the system shown in Fig. 5.

| $R_L$ [Ω] | $L_L$ [mH] | $C_L$ [μF] |
|---|---|---|
| 1.0 | 0.25 | 0.5 |

**Table 3**
Load powers for the GSMA/VD simulations.

| $t$ [ms] | $P_2^*$ [W] | $P_3^*$ [W] | $P_4^*$ [W] | $P_5^*$ [W] |
|---|---|---|---|---|
| 0 | 0 | 0 | 0 | 0 |
| 50 | 1500 | 0 | 0 | 1500 |
| 100 | 1500 | 3000 | 0 | 1500 |
| 150 | 1500 | 3000 | 2250 | 1500 |

The parameters of the lines that are used in the simulation are given in Table 2.

A droop source is situated at $n_1$, which has a reference voltage of ±350 V and a droop impedance of 140 W/V. Furthermore, two constant power loads, controlled with the GSMA/VD algorithm, are situated at the other nodes and their reference powers over time are given in Table 3.

### 4.2. Scenario without demand response

For the first simulation, the pole-to-pole voltage at which the constant power load converters switch off is configured as 630 V (±315 V). The node voltages, as a result of the given scenario, are shown in Fig. 6. For clarity's sake, and because the system is symmetrical, only the positive pole quantities are displayed. In the figure, the loads at nodes $n_2$ to $n_5$ are indicated with $L_2$ to $L_5$.

From Fig. 6, it is seen that the system remains stable, and that the voltage remains above the set value. In this case, no demand response is required from any of the GSMA/VD controllers. The only visible effect of the GSMA/VD controllers is the difference of the (short) initial delay at around 50 ms when loads $L_2$ and $L_5$ are switched on. This difference is caused by the stochastic nature of the GSMA/VD controllers.

### 4.3. Scenario with demand response

For the second simulation, the pole to pole voltage at which the load converters are disconnected is changed to 675 V (±337.5 V). The

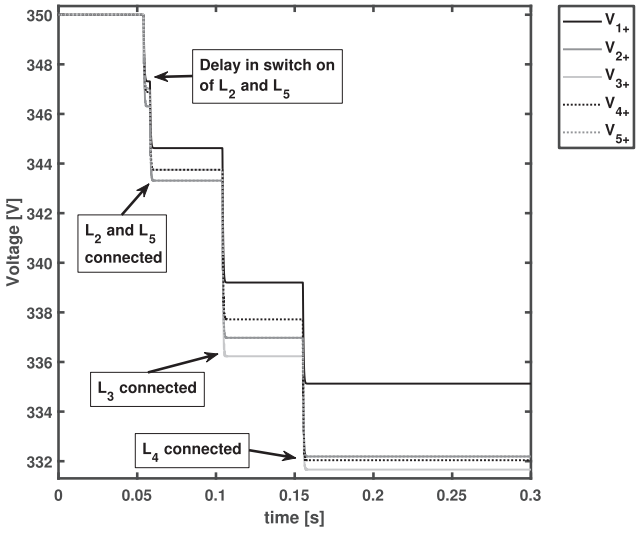


**Fig. 6.** Node voltages for the system in Fig. 5 and the scenario in Table 3, when demand response is not required.

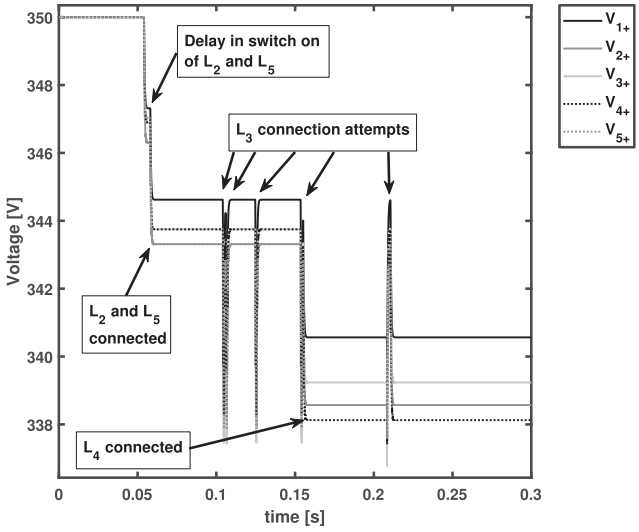


**Fig. 7.** Node voltages for the system in Fig. 5 and the scenario in Table 3, when demand response is required.

simulation results for the positive pole node voltages are shown in Fig. 7. In this scenario, demand response is required to ensure that the system remains above the desired minimum voltage. In this case, load $L_3$ cannot connect to the grid as this would lead to unacceptably low voltages.

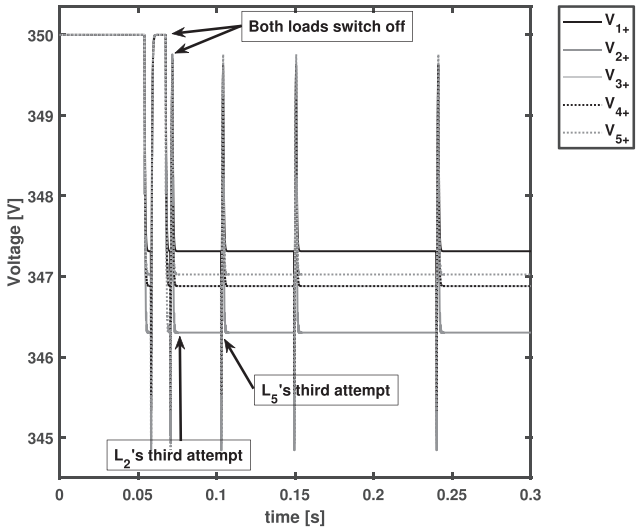


**Fig. 8.** Node voltages for the system in Fig. 5 and the scenario in Table 3, when two loads are connected simultaneously.

From Fig. 7, several observations can be made on the algorithm's behavior in a scenario where demand response needs to be applied. First, a small difference in the delay of loads $L_2$ and $L_5$ can again be seen around 50 ms. Second, at around 100 ms, the load at $n_3$ cannot be switched on since this brings the voltage at $n_3$ below ±337.5 V. Therefore, this load attempts to connect 5 times at increasing intervals, after which the connection is aborted. Third, the source can supply power to load $L_4$ without the voltage dropping below ±337.5 V. Load $L_4$ is shortly interrupted at 210 ms because of the last attempted connection of load $L_3$. However, load $L_4$ recovers quickly since the time it was connected exceeds the reset time, $T_r$, of 25 ms.

### 4.4. Scenario with simultaneous connection

The last simulation is designed to illustrate the behavior of the GSMA/VD algorithm when two loads, which have the same voltage threshold, attempt connection at the same time. Such a scenario can occur, for example after a blackout. For this simulation, only loads $L_2$ and $L_5$ are operated, and the pole to pole voltage at which the loads are disconnected is changed to 690 V (±345 V). Under these conditions, only one of these identical loads can be supplied by the source. Since both loads have the same priority, which converter remains connected to the grid is random. The simulation results for the positive pole node voltages are shown in Fig. 8.

At 50 ms, the converters attempt connections at roughly the same time twice and therefore both fail to connect. However, at around 75 ms the load $L_2$ attempts connection significantly earlier than load $L_5$ and therefore the reset time is exceeded. Consequently, after the next three connection attempts of load $L_5$, load $L_2$ recovers quickly and remains connected. Nonetheless, the last three unsuccessful connection attempts of load $L_5$ cause short interruptions in the operation of load $L_2$.

## 5. GSMA/VD experimental results

In this section the behavior of the GSMA/VD algorithm is validated by conducting experiments on a laboratory scale dc microgrid. Four experiments are conducted to show the algorithm's behavior in different scenarios.

### 5.1. Experimental DC microgrid set-up

The power electronic converters in the experimental set-up consist of three parallel half-bridges, which can be operated as an ac/dc controlled rectifier or a dc/dc interleaved boost converter (depending on how the controller is programmed). The basic topology and a picture of the power electronic converters are shown in Fig. 9.

The dc microgrid set-up consists of three identical power electronic converters, which are connected to a dc bus via line emulation circuits. These line emulation circuits have a specified inductance and resistance for both the positive pole and the neutral. A simplified schematic and a picture of the experimental set-up is shown in Fig. 10.

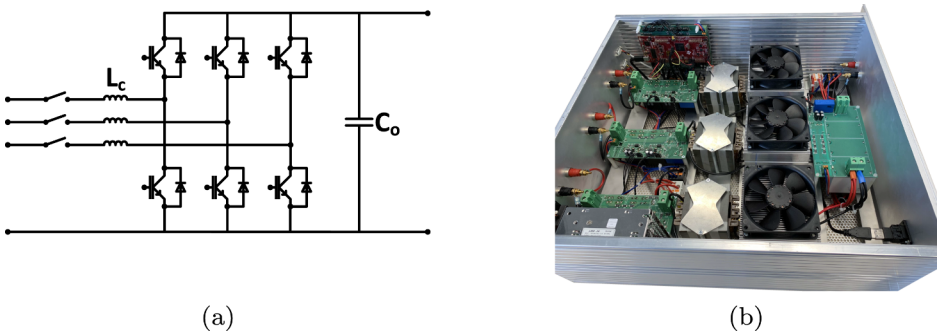


**Fig. 9.** (a) Topology of the converters, (b) Picture of the converters.

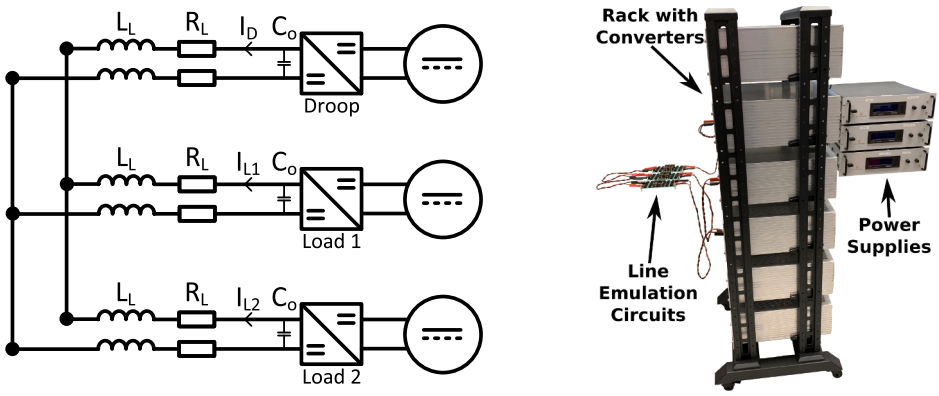


**Fig. 10.** (a) Schematic of the experimental set-up, (b) Picture of the experimental set-up.

**Table 4**
Parameters of the converters and lines in the experimental set-up.

| $L_c$ [$\mu$H] | $C_o$ [$\mu$F] | $R_L$ [$\Omega$] | $L_L$ [$\mu$H] |
|---|---|---|---|
| 430 | 250 | 0.12 | 32 |

During the experiments, the three converters are operated as dc/dc interleaved boost converters. One of the converters, labeled throughout the section as “Droop”, implements a power droop control with a reference voltage of 350 V. The two other converters, labeled “Load 1” and “Load 2”, are programmed to exhibit constant power load behavior with a power of 2.5 kW each.

In this section, the droop converter is operated with a reference voltage of 350 V and a droop constant of 250 W/V, unless otherwise specified. Furthermore, the two load converters are operated as 2.5 kW constant power loads with GSMA/VD controllers. Moreover, the voltage at which the GSMA/VD algorithm disconnects the load converters is set to 325 V. Furthermore, the parameters of the converters' input inductor and output capacitor, and the parameters of the connection to the bus are depicted in Table 4.

### 5.2. Disconnection of a single load

For the first experiment only one load is connected to the dc microgrid, while the other load remains non-operational. The droop constant of the droop converter is then reduced from 250 W/V to 75 W/V at $t = 0.1$ s. The resulting output voltage of the droop converter and the output currents from all the converters are shown in Fig. 11.

Observe that, at $t = 0.1$ s, Load 1 attempts reconnection up to seven times with increasing intervals between attempts. Finally, the connection is completely aborted and the system is left in steady state without

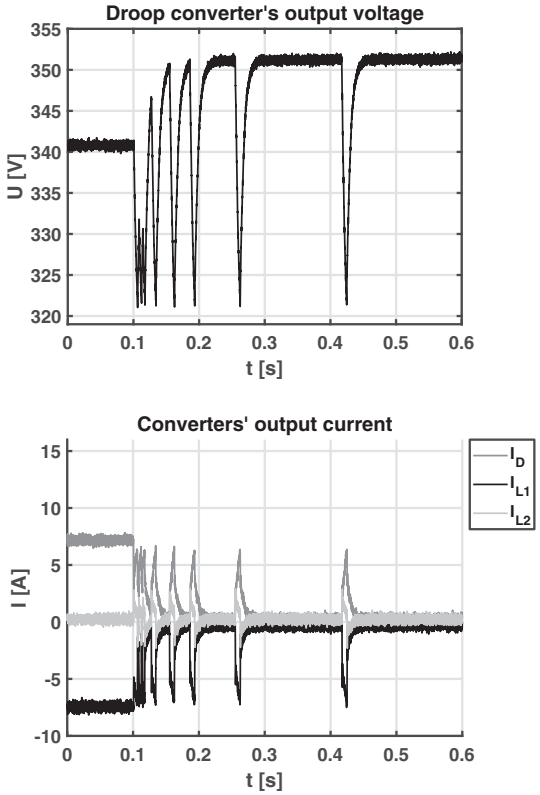


**Fig. 11.** Experimental results for one disconnecting load utilizing the GSMA/VD algorithm.

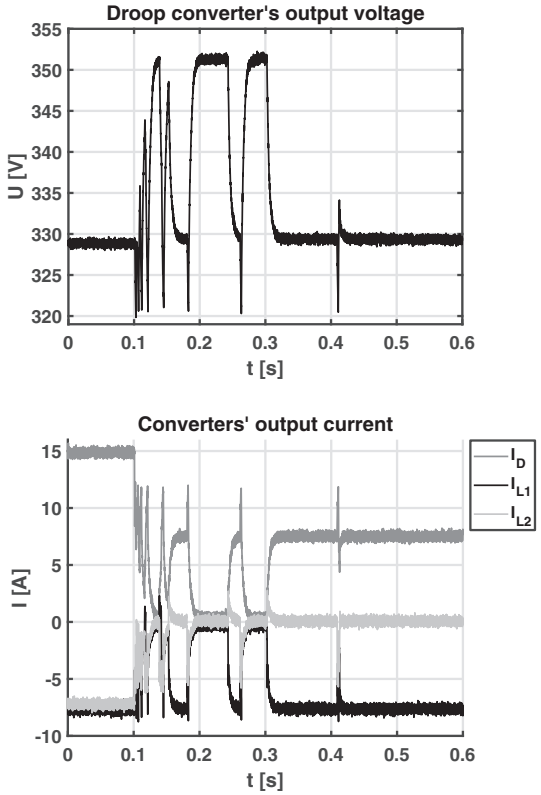


**Fig 12.** Experimental results for two loads with the GSMA/VD algorithm of which only one can remain connected to the grid.

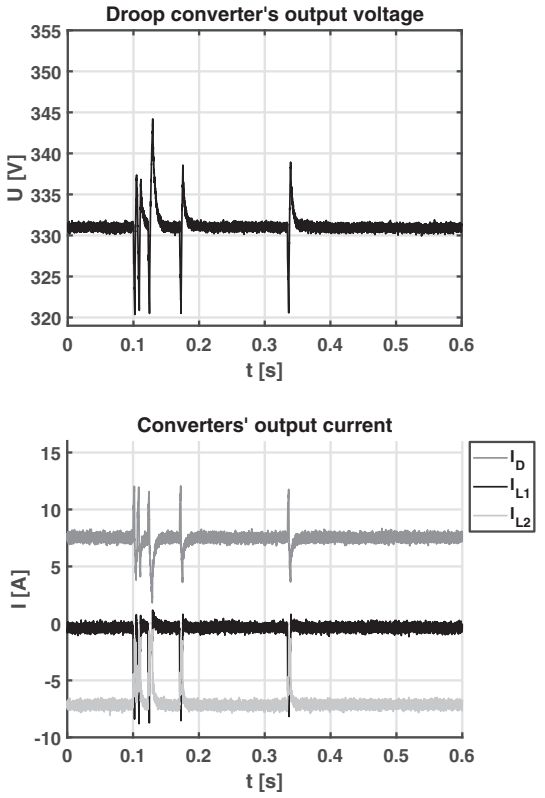


**Fig. 13.** Experimental results for two loads with the GSMA/VD algorithm showing the priority of an already connected converter.

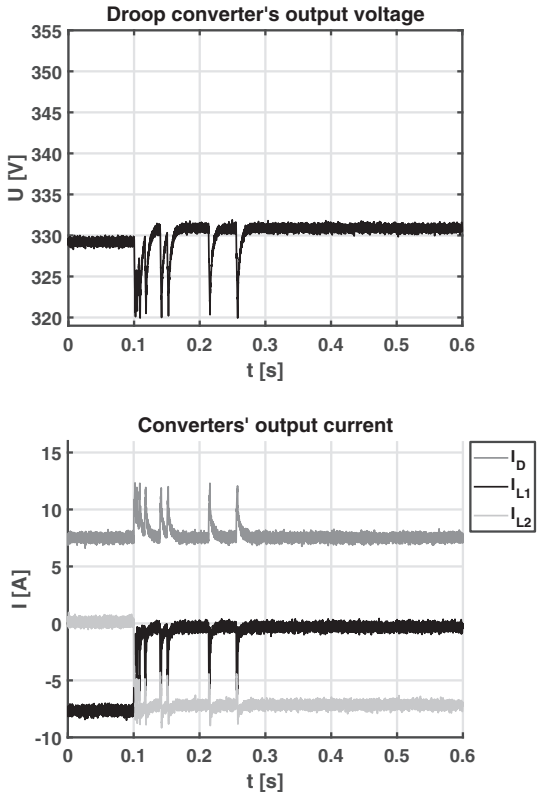


**Fig. 14.** Experimental results for two loads with the GSMA/VD algorithm when the priority is set by the voltage at which they switch off.

the load connected at a voltage of 350 V.

### 5.3. Demand response of two loads with equal priority

For the second experiment, both loads are connected to the dc microgrid. Subsequently, the droop constant is reduced from 250 W/V to 125 W/V at $t = 0.1$ s. The experimental results for this scenario are shown in Fig. 12.

When the droop constant reduces at t = 0.1 s neither of the converters are able to connect successfully to the grid at first. However, around 0.3 s Load 1 is successfully connected for more than 25 ms. Therefore, the number of connection attempts for Load 1 is reset and it remains connected after Load 2 reaches its maximum number of attempts.

### 5.4. Priority according to the connection status

For the third experiment, the droop constant of the droop converter is kept at 125 W/V during the experiment. Load 2 is successfully connected to the grid, after which Load 1 attempts connection at t = 0.1 s. The droop converter's output voltage and all the converters output currents are shown in Fig. 13.

Note that, due to the choice in $S$ and $R$, the GSMA algorithm gives priority to converters which are already connected to the grid. However, it is important to note that this is only the case if they have the same priority in terms of the voltage at which they switch off, which will be shown in the last experiment.

### 5.5. Priority according to the voltage limit

For the last experiment, the droop constant of the droop converter is again kept at 125 W/V during the experiment. The threshold voltage at which Load 2 switches off is changed to 320 V, while that of Load 1 remains at 325 V. Load 1 is successfully connected to dc microgrid first, after which Load 2 is switched on at t = 0.1 s. The results of this experiment are shown in Fig. 14.

Observe that, although the GSMA algorithm enables decisions to be made when converters of equal priority are connected, the priority of converters is still primarily determined by the voltage at which they switch off. In the experiment, Load 1 detects an undervoltage when Load 2 attempts connection, while Load 2 does not. Therefore, Load 1 attempts to reconnect until its maximum number of attempts is reached.

## 6. Conclusion

In this paper it was experimentally shown that inadequate energy utilization arises from the use of decentralized control algorithms, for example, when voltage dependent demand and supply response is applied. When the proposed GSMA algorithm is used, energy utilization is improved by allowing a subset of converters with the same voltage threshold to remain connected, without the need of utilizing any form of communication. Moreover, the behavior of the GSMA algorithm was validated using simulations and experiments.

In this paper it was shown that the GSMA algorithm can take care of the decision-making process for supply and demand response without utilizing communication. The authors expect that, with some modifications, the algorithm can also be applied to ac grids. In that case, the

frequency is also measured locally, in addition to the voltage, and the loads are disconnected if the voltage or frequency drops below its threshold. However, more simulation and experimental results are required to prove its effectiveness in ac grids.

## CRediT authorship contribution statement

**Nils H. van der Blij:** Conceptualization, Methodology, Investigation, Writing - original draft. **Laura M. Ramirez-Elizondo:** Supervision, Resources, Writing - review & editing. **Matthijs T.J. Spaan:** Supervision, Visualization, Writing - review & editing. **Pavol Bauer:** Supervision, Project administration, Funding acquisition.

## Declaration of Competing Interest

The authors declare that they have no known competing financial interests or personal relationships that could have appeared to influence the work reported in this paper.

## Appendix A. Supplementary material

Supplementary data to this article can be found online at https://doi.org/10.1016/j.ijepes.2020.105818.

## References


[1] Ipakchi A, Albuyeh F. Grid of the future. IEEE Power Energ Mag 2009;7(2):52–62. https://doi.org/10.1109/MPE.2008.931384.

[2] Bidram A, Davoudi A. Hierarchical structure of microgrids control system. IEEE Trans Smart Grid 2012;3(4):1963–76. https://doi.org/10.1109/TSG.2012.2197425.

[3] Lo C, Ansari N. Decentralized controls and communications for autonomous distribution networks in smart grid. IEEE Trans Smart Grid 2013;4(1):66–77. https://doi.org/10.1109/TSG.2012.2228282.

[4] Pepermans G, Driesen J, Haeseldonckx D, Belmans R, Dhaeseleer W. Distributed generation: definition, benefits and issues. Energy Policy 2005;33(6):787–98. https://doi.org/10.1016/j.enpol.2003.10.004.

[5] Alagoz BB, Keles C, Kaygusuz A. Towards energy webs: Hierarchical tree topology for future smart grids. 2015 3rd International Istanbul Smart Grid Congress and Fair (ICSG) 2015. p. 1–4. https://doi.org/10.1109/SGCF.2015.7354931.

[6] Kim J, Cho S, Shin H. Advanced power distribution system configuration for smart grid. IEEE Trans Smart Grid 2013;4(1):353–8. https://doi.org/10.1109/TSG.2012.2233771.

[7] Hatziargyriou N, Asano H, Iravani R, Marnay C. Microgrids. IEEE Power Energ Mag 2007;5(4):78–94. https://doi.org/10.1109/MPAE.2007.376583.

[8] Driesen J, Visscher K. Virtual synchronous generators. 2008 IEEE power and energy society general meeting - conversion and delivery of electrical energy in the 21st century 2008. https://doi.org/10.1109/PES.2008.4596800.

[9] Morren J, de Haan SWH, Ferreira JA. Contribution of dg units to primary frequency control. 2005 international conference on future power systems 2005. p. 6. https://doi.org/10.1109/FPS.2005.204253.

[10] van der Blij N, Ramirez-Elizondo L, Spaan M, Bauer P. Stability of dc distribution systems: An algebraic derivation. Energies 2017;10:1412. https://doi.org/10.3390/en10091412.

[11] Olivares DE, Mehrizi-Sani A, Etemadi AH, Caizares CA, Iravani R, Kazerani M, et al. Trends in microgrid control. IEEE Trans Smart Grid 2014;5(4):1905–19. https://doi.org/10.1109/TSG.2013.2295514.

[12] Dimeas AL, Hatziargyriou ND. Operation of a multiagent system for microgrid control. IEEE Trans Power Syst 2005;20(3):1447–55. https://doi.org/10.1109/TPWRS.2005.852060.

[13] Guerrero JM, Chandorkar M, Lee T, Loh PC. Advanced control architectures for intelligent microgridsÃ¹part i: Decentralized and hierarchical control. IEEE Trans Ind Electron 2013;60(4):1254–62. https://doi.org/10.1109/TIE.2012.2194969.

[14] Etemadi AH, Davison EJ, Iravani R. A decentralized robust control strategy for multi-der microgrids–part i: Fundamental concepts. IEEE Trans Power Delivery 2012;27(4):1843–53. https://doi.org/10.1109/TPWRD.2012.2202920.

[15] Morstyn T, Hredzak B, Agelidis VG. Control strategies for microgrids with distributed energy storage systems: An overview. IEEE Trans Smart Grid 2018;9(4):3652–66. https://doi.org/10.1109/TSG.2016.2637958.

[16] Lee M, Chen D, Huang K, Liu C, Tai B. Modeling and design for a novel adaptive voltage positioning (avp) scheme for multiphase vrms. IEEE Trans Power Electron 2008;23(4):1733–42. https://doi.org/10.1109/TPEL.2008.924822.

[17] Antoniadou-Plytaria KE, Kouveliotis-Lysikatos IN, Georgilakis PS, Hatziargyriou ND. Distributed and decentralized voltage control of smart distribution networks: Models, methods, and future research. IEEE Trans Smart Grid 2017;8(6):2999–3008. https://doi.org/10.1109/TSG.2017.2679238.

[18] Wang X, Li YW, Blaabjerg F, Loh PC. Virtual-impedance-based control for voltage-source and current-source converters. IEEE Trans Power Electron 2015;30(12):7019–37. https://doi.org/10.1109/TPEL.2014.2382565.

[19] Gu Y, Xiang X, Li W, He X. Mode-adaptive decentralized control for renewable dc microgrid with enhanced reliability and flexibility. IEEE Trans Power Electron 2014;29(9):5072–80. https://doi.org/10.1109/TPEL.2013.2294204.

[20] Mahmood H, Michaelson D, Jiang J. Reactive power sharing in islanded microgrids using adaptive voltage droop control. IEEE Trans Smart Grid 2015;6(6):3052–60. https://doi.org/10.1109/TSG.2015.2399232.

[21] Van Der Blij NH, Ramirez-Elizondo LM, Spaan MTJ, Bauer P. Stability and decentralized control of plug-and-play dc distribution grids. IEEE Access 2018;6:63726–36. https://doi.org/10.1109/ACCESS.2018.2875758.

[22] Tucci M, Riverso S, Vasquez JC, Guerrero JM, Ferrari-Trecate G. A decentralized scalable approach to voltage control of dc islanded microgrids. IEEE Trans Control Syst Technol 2016;24(6):1965–79. https://doi.org/10.1109/TCST.2016.2525001.

[23] Cingoz F, Elrayyah A, Sozer Y. Plug-and-play nonlinear droop construction scheme to optimize islanded microgrid operations. IEEE Trans Power Electron 2017;32(4):2743–56. https://doi.org/10.1109/TPEL.2016.2574202.

[24] Vasquez JC, Guerrero JM, Miret J, Castilla M, de Vicua LG. Hierarchical control of intelligent microgrids. IEEE Ind Electron Magazine 2010;4(4):23–9. https://doi.org/10.1109/MIE.2010.938720.

[25] Che L, Shahidehpour M, Alabdulwahab A, Al-Turki Y. Hierarchical coordination of a community microgrid with ac and dc microgrids. IEEE Trans Smart Grid 2015;6(6):3042–51. https://doi.org/10.1109/TSG.2015.2398853.

[26] Alagoz BB, Kaygusuz A, Karabiber A. A user-mode distributed energy management architecture for smart grid applications. Energy 2012;44(1):167–77https://linkinghub.elsevier.com/retrieve/pii/S0360544212005038https://doi.org/10.1016/j.energy.2012.06.051.

[27] Tsikalakis AG, Hatziargyriou ND. Centralized control for optimizing microgrids operation. 2011 IEEE Power and energy society general meeting 2011. p. 1–8. https://doi.org/10.1109/PES.2011.6039737.

[28] Ieee standards for local area networks: Carrier sense multiple access with collision detection (csma/cd) access method and physical layer specifications, ANSI/IEEE Std 802.3-1985, 1985. https://doi.org/10.1109/IEEESTD.1985.82837.

[29] Kwak B-J, Song N-O, Miller LE. Performance analysis of exponential backoff. IEEE/ACM Trans Netw 2005;13(2):343–55. https://doi.org/10.1109/TNET.2005.845533.

[30] Haas ZJ, Deng Jing. On optimizing the backoff interval for random access schemes. IEEE Trans Commun 2003;51(12):2081–90. https://doi.org/10.1109/TCOMM.2003.820754.

[31] van der Blij NH, Ramirez-Elizondo LM, Spaan MTJ, Bauer P. A state-space approach to modelling dc distribution systems. IEEE Trans Power Syst 2018;33(1):943–50. https://doi.org/10.1109/TPWRS.2017.2691547.